Adaptive introgression during environmental change can weaken reproductive isolation

Gregory L. Owens [1]* and Kieran Samuk [2]

Anthropogenic climate change is an urgent threat to species diversity[1,2]. One aspect of this threat is the merging of species through increased hybridization[3]. The primary mechanism for this collapse is thought to be the weakening of ecologically mediated reproductive barriers, as demonstrated in cases of 'reverse speciation'[4,5]. Here, we expand on this idea and show that adaptive introgression between species adapting to a shared, moving climatic optimum can readily weaken any reproductive barrier, including those that are completely independent of climate. Using genetically explicit forward-time simulations, we show that genetic linkage between alleles conferring adaptation to a changing climate and alleles conferring reproductive isolation (intrinsic and/or non-climatic extrinsic) can lead to adaptive introgression facilitating the homogenization of reproductive isolation alleles. This effect causes the decay of species boundaries across a broad and biologically realistic parameter space. We explore how the magnitude of this effect depends on the rate of climate change, the genetic architecture of adaptation, the initial degree of reproductive isolation, the degree to which reproductive isolation is intrinsic versus extrinsic and the mutation rate. These results highlight a previously unexplored effect of rapid climate change on species diversity.

One potential effect of global climate change (GCC) is increased interspecies hybridization by, for example, bringing together species ranges or disrupting mating timing[4]. Such hybridization can cause a common species to subsume a rare species[6] or the collapse of multiple species into a single hybrid swarm[7]. In both cases, species diversity is lost, as has been seen in smaller localized environmental shifts[5,7].

There is a rich theoretical literature dedicated to the study of the dynamics of interspecific hybridization (reviewed in, for example, refs. [8–10]). However there has thus far been poor integration between models of reproductive isolation (RI) and models of adaptation to climate change. The fact that introgression can transfer alleles between species has led to the idea that hybridization could facilitate adaptation to GCC through the transfer of adaptive alleles between species—that is, adaptive introgression. This has traditionally been studied in the context of species/populations with pre-existing differential adaptation to the changing climate variable; for example, a warm-adapted species transferring alleles to a cold-adapted species[11]. In this example, one species acts as a pool of alleles preadapted to a future climatic optimum. Importantly, in these types of models, introgression is being driven by selection and not demographic processes or perturbations of prezygotic isolation, as seen in other models where climate change drives hybridization.

What has not been appreciated in previous models of adaptation to a changing climate is that during a rapid environmental shift, segregating variation within two reproductively isolated species could theoretically undergo adaptive introgression even if neither species is particularly preadapted to the environmental shift. We propose that climate-induced adaptive introgression could readily occur in most species because (1) the identities of the particular alleles involved in climatic adaptation are likely idiosyncratic in each species/population and (2) these alleles could, in principle, be globally adaptive under a GCC scenario. Indeed, segregating climate adaptation alleles (or linked blocks of alleles) could easily be strong enough to outweigh the fitness costs of any linked RI alleles. As a side effect, RI alleles could readily be homogenized between species, reducing RI and precipitating the collapse of species boundaries. This scenario dramatically increases the likelihood of GCC-induced introgression from populations differing in altitude or latitude to nearly any parapatric pair capable of hybridization, even if RI is initially high.

Here, we directly test the role of climate-induced adaptive introgression in degrading reproductive barriers using state-of-the-art forward-time population genetic computer simulations (Supplementary Fig. 1 and Methods). We consider the scenario of two parapatric species inhabiting demes in two different habitats. These species exchange migrants at a low level, but RI via local adaptation (that is, extrinsic postzygotic isolation and immigrant inviability) is strong enough to prevent substantial introgression. We imagine that these two species must also cope with constant adaptation to a shared oscillating 'climate' optimum. This climatic optimum does not directly affect the degree of local adaptation and/or RI; that is, RI is completely independent of the direct effects of climate. The climate oscillation continues for a long initial burn-in period, during which alleles conferring adaptation to climate (that is, climate-related quantitative trait loci (QTL)) accumulate in each species. After this period, the oscillation ends and the climatic optimum begins rapidly increasing at a constant rate (Δ per generation), as is expected under projections of anthropogenic climate change. We then measure the amount of RI lost at the end of the climate change period compared with a control period of the same length. With our simulations we ask three questions: (1) Can climate change drive RI collapse, and what factors control its severity? (2) To what extent does introgression facilitate adaptation to climate change? (3) Do the latter two phenomena occur under realistic evolutionary conditions?

When climate change is rapid, we find that adaptive introgression of climate QTL alleles rapidly drives the homogenization of allele frequencies at linked RI loci between species. Figure 1 visualizes one example simulation where, after 100 generations of climate change, RI is degraded to nearly half its original strength (Fig. 1a) and introgressed climate QTL alleles are common (Fig. 1b). As climate QTL alleles move between populations, RI and neutral alleles hitchhike

[1]Department of Integrative Biology, University of California, Berkeley, Berkeley, CA, USA. [2]Department of Biology, Duke University, Durham, NC, USA.
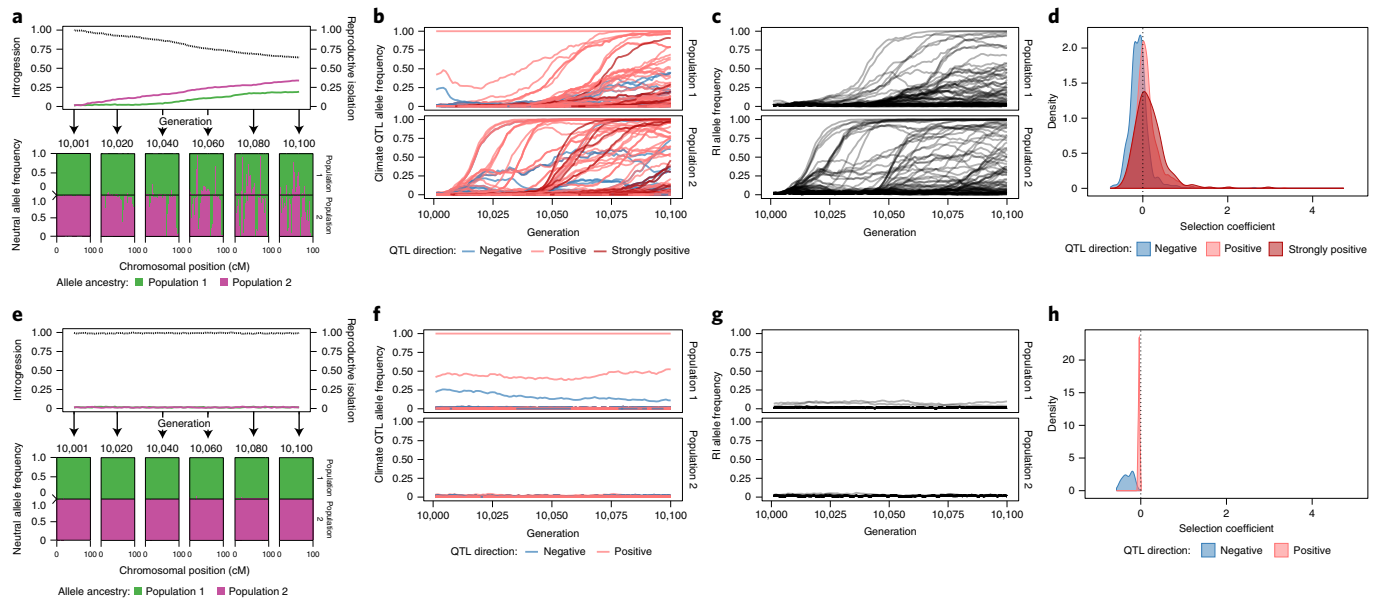*e-mail: gregory.lawrence.owens@gmail.com

Fig. 1 | An example simulation with $\Delta = 1.5$ illustrating climate-driven adaptive introgression. a–h, Panels **a–d** present the test climate change scenario, while **e–h** are the control scenario. **a,e,** The upper half of each panel is the average introgressed ancestry for each species and the average RI between populations (black). The lower half is the ancestry for neutral loci during the post-burn-in period at 20-generation intervals. The top and bottom parts of this portion represent species 1 and 2, respectively. **b,f,** The allele frequency trajectory for introgressed climate QTL colour coded by QTL strength. Colour codes of the QTL effect: negative phenotypic effects, positive effects or large positive effects (>2). **c,g,** The allele frequency trajectory for introgressed RI alleles. **d,h,** The distribution of selection coefficients on QTL loci per species per generation. Colour groups represent QTL with negative phenotypic effects, positive effects or large positive effects (>2). Plots are filtered to include only loci with allele frequency <0.9 and >0.1.

along with them, resulting in substantial genome-wide introgression (Fig. 1a,c). In contrast, in the control scenario without climate change, RI remains intact and introgression is minimal (Fig. 1e–h).

For a wide range of parameter values, we find decreased RI and increased introgressed ancestry under the climate change scenario (Fig. 2 and Supplementary Fig. 2). When adaptive variation is limited, when RI is initially weak or when environmental change is rapid, then complete genetic homogenization is likely. In these cases, RI is completely degraded and would clearly represent speciation reversal in a natural system. In other cases, introgression is increased during environmental change, but populations do not completely homogenize (Supplementary Fig. 2). In these cases, RI is still eroded between populations (Fig. 2). We believe that our estimates of RI loss are probably conservative, because we do not include any additional factors that would contribute to species collapse (for example, cases where RI is directly affected by a change in climate).

We found that, in the absence of divergent selection, intrinsic RI (due to Bateson–Dobzhansky–Muller (BDM) incompatibilities) was unable to maintain RI during the burn-in period. This result is consistent with previous modelling of parapatric speciation[12,13]. Consistent with their effect in the burn-in period, during climate change, introgression and RI loss is enhanced when RI is purely intrinsic. While other forms of intrinsic isolation that are more resistant to introgression have been suggested[14], any intrinsic isolation locus can be weakened by introgression. In contrast, the strength of an extrinsic isolation locus is independent of genomic background, and as such we do not expect any form of intrinsic isolation to be more resistant to the adaptive introgression than the extrinsic isolation modelled here (assuming similar genomic architecture). Thus, although we have focused on extrinsic RI, intrinsic RI is also susceptible to adaptive introgression.

The ultimate question of which species are in danger of reverse speciation is dependent on a multitude of interacting factors, but based on our simulations we can highlight several risk factors:

(1) The potential for hybridization. Surveys have estimated the percentage of species that hybridize with at least one other congener to be around 10–25%, although if climate change disrupts species ranges or premating isolation, that number may increase[15].

(2) The rate of environment change and the steepness of the changing fitness landscape. Species with broader climate niches will be less susceptible because they will be under weaker selection.

(3) The genetic architecture of climate adaptation within species. Species with numerous large-effect climate adaptation alleles segregating within their gene pool will be more able to adapt to the changing climate without introgressed alleles. Low-diversity species will be more susceptible to adaptive introgression.

(4) The genetic architecture of RI between species. Species with few large-effect RI loci will be more resistant to RI decay than species with a more diffuse and polygenic RI architecture. See the Supplementary Discussion for further exploration of the role of linkage and recombination rate.

(5) The demographic and life history of the species. Unbalanced population sizes may result in one population harbouring more adaptive alleles and lead to unbalanced introgression. Small populations will also be more susceptible to extinction due to the fitness costs of introgressed RI alleles. Features that reduce effective population size, for example, high variance in reproductive success, are also likely to have reduced diversity of climate-adapting alleles.

Our simulations suggest that rapidly changing environments can cause the collapse of species barriers even when the mechanisms of RI are independent of climate. We modelled a scenario in which the strength of RI (modelled as divergent selection) is (1) invariant throughout (that is, not reduced by environmental change itself) and (2) orthogonal to the strength of climate-mediated selection (that is, extrinsic RI alleles do not affect the climate phenotype). This is an
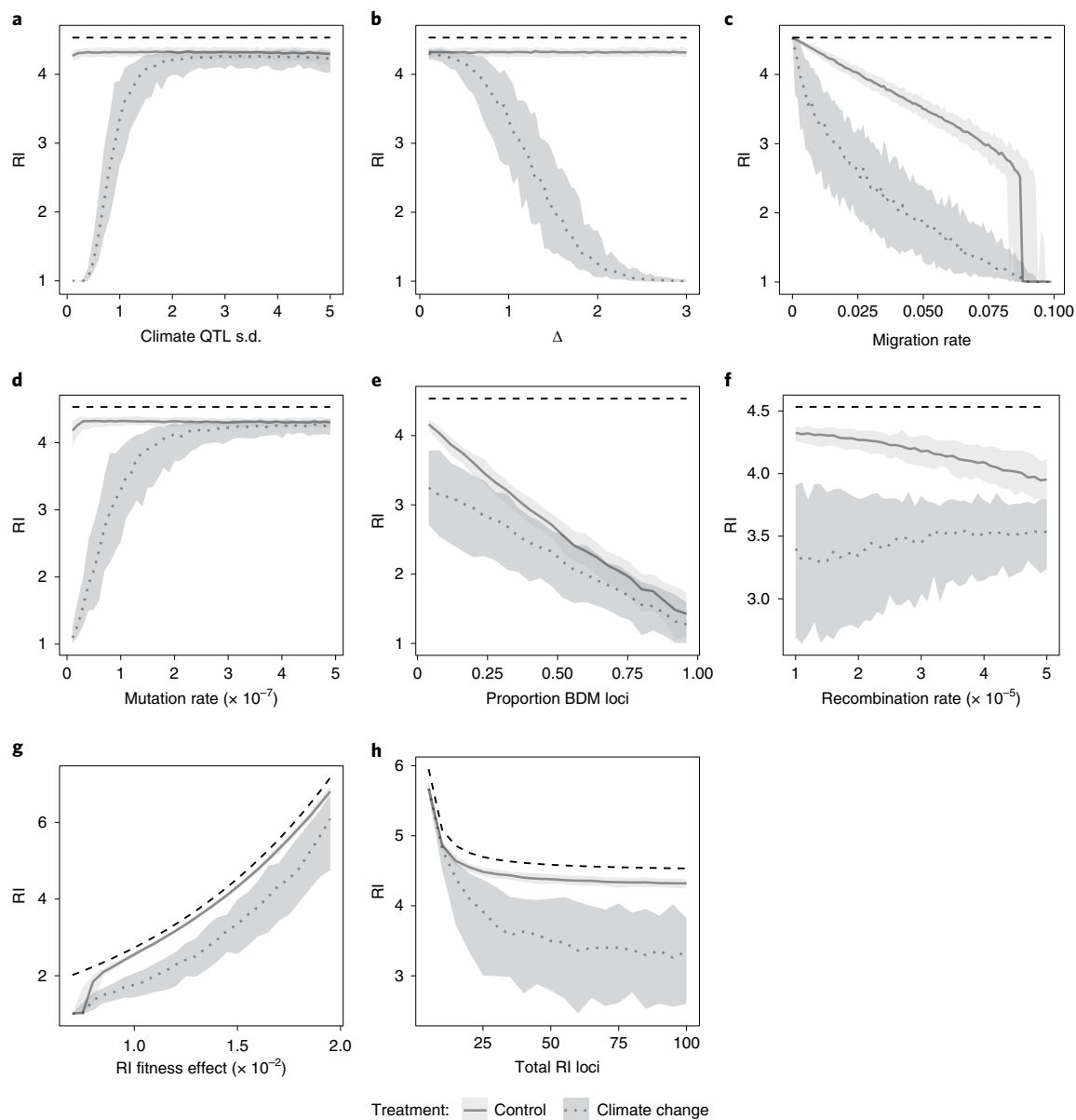
Fig. 2 | The effect of simulation parameters on RI loss. a–h, The average RI at generation 10,100 for climate change and control simulations while varying individual parameters. The shaded areas encompass 95% of the simulations of each treatment. RI is defined as the home fitness advantage, which is the n-fold fitness advantage for the average sample in its home environment compared with the alternative environment based on divergent selection and BDM loci. A value of 1 means equal fitness in both environments and no RI. The dashed line is the initial and maximum level of RI for each simulation. Individual parameters were varied to show the effects of climate QTL effect-size s.d. (**a**), optimum shift per generation (Δ) (**b**), migration rate (**c**), climate QTL mutation rate (**d**), proportion of RI loci that are BDM instead of extrinsic (**e**), the recombination rate (**f**), the fitness effect of each RI locus (**g**) and the number of RI loci (**h**).

important departure from previous work, in which the collapse of RI or 'reverse speciation' occurs because RI is itself dependent on the environment (for example, trophic or sensory niche[5]).

This difference in modelling approach has several important implications. For one, the collapse of RI we describe here can occur in any population where adaptive introgression is possible (that is, RI is not absolute, and the climate-mediated selective optimum is, to some degree, shared). This greatly expands both the number of populations that may be susceptible to introgressive collapse and the potential severity of such collapses. For example, adaptive introgression could act in concert with the collapse of climate-mediated reproductive barriers or a reduction in population sizes, accelerating reverse speciation.

Although we have framed our discussion in the context of climate change, our results are applicable to any strong, consistent and shared selective event. These events include any environmental or ecological disturbance that alters the shared selective landscape of species such that they are sufficiently displaced from their selective optima (that is, selection is sufficiently strong). One such event that has been studied in natural systems is eutrophication, which has been suggested to have caused speciation reversal in European lake whitefish[5]. Thus far, this reversal has been attributed to changes in RI as a direct result of ecological and/or behavioural changes. However, if eutrophication exerts a common selective pressure on a group of parapatric species (for example, mediated through changes in water chemistry) introgression could become adaptive and
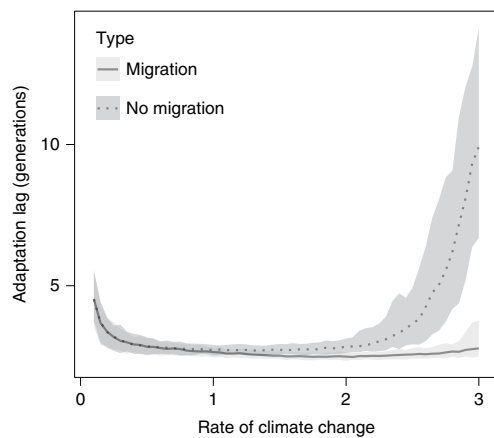
Fig. 3 | Hybridization enhances adaptation at high rates of climate change. The adaptational lag at the final generation for simulations with migration (that is, with hybridization; $m = 0.01$) and without migration (that is, with hybridization; $m = 0$). The shaded areas encompass 95% of the simulations of each type. Adaptational lag is defined as the phenotypic optimum minus the phenotypic mean divided by the rate of climate change, and it represents how many generations behind the changing optimum that the population is.

contribute to the collapse of species boundaries. Similarly, ocean acidification could be a strong source of shared selection and may induce introgression between previously well-isolated species[16].

While we focus our discussion on how introgression can lead to species merging together, it is likely that the adaptive introgression of climate QTL also increases the chance that one or both species can adapt to a changing environment and avoid extinction. We cannot directly address this question in our model (Supplementary Discussion) but we do see that when all introgression is prevented, the lag between the current phenotype and the current optimum increases (Fig. 3). This is consistent with the larger total gene pool of adaptive variants available when gene flow is possible. We see this effect most strongly when climate change is rapid, suggesting the benefits of introgression mainly occur when adaptation is most challenging.

A strong shared selection pressure is ultimately the key mediator of the collapse of RI we observed. Was the magnitude of simulated selection necessary to cause this collapse realistic? One way to assess this is to measure the magnitude of the phenotypic response to selection in our simulations and compare it with estimates from natural systems. In our case, the phenotypic response to selection ranged from 0.01 to 0.06 haldanes (a measure of evolutionary rate; s.d. per generation) (Supplementary Fig. 3). This is in line with the magnitude of phenotypic response observed in both natural and anthropogenically induced selection[17]. Further, this is well below the theoretical threshold of 0.1 haldanes thought to result in an unsustainable long-term response to selection (for an effective population size of $N_e = 500$; refs. [18,19]).

Another way of assessing the realism of our scenarios is comparing the selection coefficients of climate QTL in our simulations with values measured in empirical studies. We measured selection coefficients in our example simulation by comparing relative fitness values for samples with and without each locus (Supplementary Methods). Only 0.7% of introgressed climate QTL loci had selection coefficients >1, again indicating that they were well within the range of natural estimates[20]. Thus, the strength of selection we modelled was in no way extreme nor would it necessarily lead to the extinction of the populations under natural conditions. It is also worth noting that the estimated rates of phenotypic change in wild populations due to future GCC are thought to be at least as large

as the rates we described here, and they are projected to probably exceed 0.1 haldanes in many cases[21,22]. In sum, the global strength of phenotypic selection simulated here was not unrealistically high and represents, if anything, a conservative adaptive scenario.

Hybridization is a double-edged sword under rapid environmental change. It can provide species access to a larger pool of adaptive alleles, but these alleles may be linked to RI alleles, weakening RI and potentially leading to speciation reversal. Our work highlights the dangers of hybridization for a much wider pool of species, not just those on range margins or with existing porous species boundaries. In the longer term, we predict that specific cases of speciation reversal should be linked to climate change, but we also predict effects other than speciation reversal. One core prediction of our model is that alleles conferring adaptation to a shared climate will be more likely to introgress between species. Although identifying all the loci underlying climate adaptation is challenging, recent work by Exposito-Alonso et al.[23] highlights progress towards this goal. Such an approach can be combined with sequencing data in related species to identify where introgression is most likely to occur. Our results also suggest that climate change should cause hybrid zones to become increasingly porous as climate adaptation alleles move between species and that this effect would be stronger in regions with more dramatic climate change (for example, Arctic regions[24]). This prediction could be tested by resampling previously studied hybrid zones or by comparing contemporary samples with museum and herbarium samples. Confirmation of these predictions would show that climate adaptation is occurring through a larger multi-species gene pool and be a warning sign for the future homogenization of these species.

Online content

Any methods, additional references, Nature Research reporting summaries, source data, extended data, supplementary information, acknowledgements, peer review information; details of author contributions and competing interests; and statements of data and code availability are available at https://doi.org/10.1038/s41558-019-0628-0.

References

1. Thomas, C. D. et al. Extinction risk from climate change. *Nature* **427**, 145–148 (2004).
2. Hoffmann, A. A. & Sgrò, C. M. Climate change and evolutionary adaptation. *Nature* **470**, 479–485 (2011).
3. Todesco, M. et al. Hybridization and extinction. *Evol. Appl.* **9**, 892–908 (2016).
4. Chunco, A. J. Hybridization in a warmer world. *Ecol. Evol.* **4**, 2019–2031 (2014).
5. Vonlanthen, P. et al. Eutrophication causes speciation reversal in whitefish adaptive radiations. *Nature* **482**, 357–362 (2012).
6. Oliveira, R., Godinho, R., Randi, E. & Alves, P. C. Hybridization versus conservation: are domestic cats threatening the genetic integrity of wildcats (*Felis silvestris silvestris*) in Iberian Peninsula? *Phil. Trans. R. Soc. Lond. B* **363**, 2953–2961 (2008).
7. Taylor, E. B. et al. Speciation in reverse: morphological and genetic evidence of the collapse of a three-spined stickleback (*Gasterosteus aculeatus*) species pair. *Mol. Ecol.* **15**, 343–355 (2006).
8. Abbott, R. et al. Hybridization and speciation. *J. Evol. Biol.* **26**, 229–246 (2013).
9. Barton, N. H. Does hybridization influence speciation? *J. Evol. Biol.* **26**, 267–269 (2013).
10. Seehausen, O. Conditions when hybridization might predispose populations for adaptive radiation. *J. Evol. Biol.* **26**, 279–281 (2013).
11. Gómez, J. M., González-Megías, A., Lorite, J., Abdelaziz, M. & Perfectti, F. The silent extinction: climate change and the potential hybridization-mediated extinction of endemic high-mountain plants. *Biodivers. Conserv.* **24**, 1843–1857 (2015).
12. Barton, N. & Bengtsson, B. O. The barrier to genetic exchange between hybridising populations. *Heredity* **57**, 357–376 (1986).

13. Bank, C., Bürger, R. & Hermisson, J. The limits to parapatric speciation: Dobzhansky–Muller incompatibilities in a continent–island model. *Genetics* **191**, 845–863 (2012).

14. Lindtke, D. & Buerkle, C. A. The genetic architecture of hybrid incompatibilities and their effect on barriers to introgression in secondary contact. *Evolution* **69**, 1987–2004 (2015).

15. Mallet, J. Hybridization as an invasion of the genome. *Trends Ecol. Evol.* **20**, 229–237 (2005).

16. Pespeni, M. H. et al. Evolutionary change during experimental ocean acidification. *Proc. Natl Acad. Sci. USA* **110**, 6937–6942 (2013).

17. Hendry, A. P., Farrugia, T. J. & Kinnison, M. T. Human influences on rates of phenotypic change in wild animal populations. *Mol. Ecol.* **17**, 20–29 (2008).

18. Lynch, M. & Lande, R. in *Biotic Interactions and Global Change* (eds Kareiva, P. M. et al.) 234–250 (Sinauer, 1993)

19. Bürger, R. & Lynch, M. Evolution and extinction in a changing environment: a quantitative-genetic analysis. *Evolution* **49**, 151–163 (1995).

20. Kingsolver, J. G. et al. The strength of phenotypic selection in natural populations. *Am. Nat.* **3**, 245–261 (2001).

21. Gienapp, P., Leimu, R. & Merilä, J. Responses to climate change in avian migration time—microevolution versus phenotypic plasticity. *Clim. Res.* **35**, 25–35 (2007).

22. Merilä, J. & Hoffmann, A. A. in *Oxford Research Encyclopedia of Environmental Science* https://doi.org/10.1093/acrefore/9780199389414.013.136 (Oxford Univ. Press, 2016)

23. Exposito-Alonso, M. et al. Genomic basis and evolutionary potential for extreme drought adaptation in *Arabidopsis thaliana*. *Nat. Ecol. Evol.* **2**, 352–358 (2018).

24. Osborne, E., Richter-Menge, J. & Jeffries, M. *Arctic Report Card 2018* (NOAA Arctic Program, 2018); https://www.arctic.noaa.gov/Report-Card

Methods

Model details. We implemented our model as a genetically explicit Wright–Fisher model in the evolutionary simulation framework SLiM 3.0 (ref. [25]). As in all Wright–Fisher models, population sizes are constant, all fitness is relative and extinction is impossible. The details of our implementation are depicted graphically in Supplementary Fig. 1, and a list of simulation parameters and their values is detailed in Supplementary Table 1. We simulated two diploid populations of constant size N_e, with a constant migration rate of m (proportion of migrants per generation). Each individual was initialized with 99,999 genetic loci contained on a single chromosome, with a uniform recombination rate of r between loci. We initially scaled the recombination rate so that the entire genome was 100 cM in length, but we also explored varying recombination rates up to a genome size of 1,000 cM. We modelled extrinsic isolation between the two populations as l_{EX} divergently selected alleles at loci evenly spaced across the chromosome, with each population fixed for a different allele. Divergently selected alleles imposed a fitness cost of s_{RI} when not found in their home population/habitat, modelling extrinsic postzygotic isolation.

In addition to extrinsic postzygotic isolation, we also modelled intrinsic postzygotic isolation using two-locus BDM incompatibilities[26–28] ('BDMs', hereafter). These epistatic incompatibilities were modelled as a fitness cost of s_{RI} scaled by the number of negatively interacting pairs of alleles from each population (Supplementary Table 2). When testing the effects of BDMs, we maintained a constant number of total RI loci, but we varied the proportion of loci that were extrinsic or BDM loci (l). We also explored the effect of the total number of RI loci (that is, the genetic architecture of RI, per se) on the potential for adaptive introgression/hybridization. To keep the total magnitude of RI similar between simulations, we always co-varied s_{RI} so that the $s_{RI} \times l$ was held constant. To allow for a fine-scale view of introgression, we tracked ancestry using 100 neutral alleles initially fixed between the populations, spread evenly across the genome. All alleles of selective or phenotypic effect were codominant, with dominance = 0.5.

In addition to RI, individual fitness also depended on the individual's phenotypic distance from a climatic optimum. This optimum was initially 0, and during the burn-in period it oscillated from −5 to 5 (in arbitrary units) every 500 generations based on the formula $\sin(\pi \times \text{generation}/500)/5$. The individual phenotype was determined by alleles at QTL-like climate loci, which could appear via mutation at all sites other than RI or ancestry-tracking loci (that is, at $99{,}899 - l$ sites). Climate QTL mutations occurred at a rate per locus per sample per generation, and their phenotypic effect was drawn from a Gaussian distribution with a mean of zero and a standard deviation of QTL$_{s.d.}$. Conceptually, these QTL climate alleles modify whether an individual is 'hot' (positive effects) or 'cold' (negative effects) adapted.

The first step of the simulations was a burn-in of $10N_e$ generations to simulate the generation of standing genetic variation under normal climatic conditions. At the end of the burn-in period, the complete state of each replicate simulation was saved. Each simulation was then continued under both a 'control' and climate change scenario for an additional 100 generations. In the control scenario, the environmental oscillation continued as normal. In contrast, under the climate change scenario, the phenotypic optimum increased by a rate of Δ each generation, without oscillation. In each generation, we recorded the average degree of RI, mean fitness, the mean and s.d. of the climate phenotype and the amount of introgressed ancestry for each population. RI was calculated accounting for the extrinsic and BDM loci. For extrinsic loci, RI was the difference in fitness for an average individual in its home habitat versus the foreign habitat. For BDMs, since fitness penalties occur only in F$_1$ hybrids and beyond, we calculated the expected average magnitude of BDM fitness costs based on Hardy–Weinberg expectations in F$_1$ hybrids. Finally, for each simulation, we report the mean introgressed ancestry and RI between the start and end of control and test scenarios, as well as the mean rate of phenotypic change in haldanes for the test scenario. A haldane is a measure of evolutionary change in log mean trait value in units of standard deviation of that log trait[29]. All formulae used in the simulation are presented below, and all code for underlying simulations is available at https://github.com/owensgl/adaptive_introgression.

To explore the parameter space under which adaptive introgression mediates RI collapse, we systematically varied the following parameters: mutation rate (μ), m, strength of divergent selection (s_{RI}), the number of divergently selected loci (n_{RI}), the proportion of BDMs (BDM$_{pr}$), QTL$_{s.d.}$, r and Δ. We varied each parameter independently and kept the other parameters at a default value known to permit a low level of introgression in preliminary tests (Supplementary Table 1). Each parameter set was replicated 100 times. All analyses were carried out in R version 3.5.1 (ref. [30]), and plotting was done using ggplot2 (ref. [31]).

Finally, while our primary goal was testing the detrimental effects of hybridization, we also examined the potential beneficial effects of climate change-induced introgression—that is, to what degree introgression facilitates adaptation. To do this, we ran simulations varying the rate of climate change with migration ($m = 0.01$) or without migration ($m = 0$). At the last generation (gen = 10,100), we compared the average climate phenotype with the phenotypic optimum. We defined 'adaptational lag' as the difference between these values divided by the rate of climate shift. This represents the number of generations of lag behind the current generation's climate conditions that the population is adapted to. For example, assume the optimum increases by 2 per generation and is currently 100; if the average phenotype is 90, then the adaptational lag is 5 (for example, $(100 - 90)/2$).

Fitness calculations. All symbols used in the following equations are described and compiled in Supplementary Table 3. Fitness in this model is determined by how well the sample's phenotype matches the current climate optimum as well as the genotypes of RI alleles. During the initial burn-in of b generations, the climate optimum oscillates slightly above and below zero, with an amplitude of a and a frequency of f (equation (1)), and then it increases linearly during the climate shift period by Δ units per generation (equation (2)).

$$O_{\text{gen}_{\text{burn}}} = \sin(\pi \times \text{gen}/f)a \qquad (1)$$

$$O_{\text{gen}_{\text{shift}}} = \Delta(\text{gen} - b) \qquad (2)$$

For each copy of a QTL allele, i, in a sample, from a total of n_{QTL} alleles, the effect sizes, Q_i, are summed to produce the sample's climate phenotype. In this way, QTLs are all additive and codominant (dominance = 0.5). The fitness effect of this phenotype was determined by a Gaussian function with a mean corresponding to the current climate optimum O_{gen} and a standard deviation of s.d.$_{\text{climate}}$ (equation (3)). Samples with climate phenotypes distant from the optimum have reduced relative fitness.

$$\omega_{\text{climate}} = f\left(\left(\sum\nolimits_{i=1}^{n_{QTL}} Q_i\right) - O_{\text{gen}} \middle| 0, \text{s.d.}_{\text{climate}}\right) \qquad (3)$$

Along with climate adaptation, fitness is also determined by the alleles at RI loci, which are either extrinsic or intrinsic epistatic. In most simulations, all RI loci were extrinsic, except in simulations designed to test the effect of BDM incompatibilities. The effect of l extrinsic RI loci was determined by summing the counts of non-local alleles (g_{away}) divided by 2 (for co-dominance) (equation (4)).

$$n_{EX} = \sum\nolimits_{i=1}^{l_{EX}} \frac{g_{\text{away}}}{2} \qquad (4)$$

BDM loci were initialized as randomly selected pairs. In each pair, both populations were initially fixed for different alleles in the simulation at l_{BDM} loci. One locus was set as the derived state (A) in population 1 and the other as the derived state (B) in population 2. Negative interactions occur when both derived alleles are present in a single diploid individual and are equally deleterious in all combinations (Supplementary Table 2). Thus each BDM pair could produce epistasis (τ), counted as 0 or 2, and this was summed for each individual (equation (5)).

$$n_{BDM} = \sum\nolimits_{i=1}^{l_{BDM}/2} \tau_i \qquad (5)$$

The total sum of divergently selected alleles n_{EX} and BDM epistasis n_{BDM} were treated as independent alleles with selection coefficients of s_{RI} and were multiplicatively added (equation (6)). This puts BDM and extrinsic alleles on the same scale so they are comparable. Although this model results in diminishing returns in terms of absolute fitness, relative fitness scales correctly.

$$\omega_{RI} = (1 - s_{RI})^{(n_{EX} + n_{BDM})} \qquad (6)$$

The two measures of fitness were combined to create the fitness measure of each sample (equation (7)).

$$\omega = \omega_{\text{climate}} \times \omega_{RI} \qquad (7)$$

RI calculations. To see whether rapid shifts in the phenotypic optimum can lead to reverse speciation, we measured average RI during the climate shift period. We operationally defined RI as the difference in fitness between an average migrant individual versus an average non-migrant (that is, the difference in expected 'home' versus 'away' fitness). This is determined purely based on the extrinsic and BDM RI alleles, and it does not include climate QTL alleles.

For extrinsic loci, we can think of the RI in terms of a representative individual being transported from its own population to the other population and measuring its relative fitness. We calculated the average 'home' fitness by measuring the proportion(p_{EX}) of foreign alleles and applying it to equation (6) to get an expected fitness penalty. This was averaged for both populations (denoted hereafter as p1 and p2) to calculate the expected average 'home' fitness score (equation (8)).

$$E(\bar{\omega}_{EX_{\text{HOME}}}) = \frac{(1 - s_{RI})^{(p_{EXp1_{\text{AWAY}}})(l_{EX})} + (1 - s_{RI})^{(p_{EXp2_{\text{AWAY}}})(l_{EX})}}{2} \qquad (8)$$

'Away' fitness was calculated in a similar way, but using the proportion of home alleles when calculating the expected fitness penalty (equation (9)).

$$E(\bar{\omega}_{EX_{\text{AWAY}}}) = \frac{(1 - s_{RI})^{(p_{EXp1_{\text{HOME}}})(l_{EX})} + (1 - s_{RI})^{(p_{EXp2_{\text{HOME}}})(l_{EX})}}{2} \qquad (9)$$

RI calculations from BDMs are more complicated, because BDMs have no effect in generation 0 after migration (that is, before breeding). Their effect only

appears after mating in F_1 hybrids and beyond, which have combinations of alleles from both populations. Thus, for BDMs, we estimated expected RI based on Hardy–Weinberg expectations of genotype frequencies (ancestral $a|b$ and derived $A|B$) assuming mating within the population and mating between populations (Supplementary Tables 4 and 5). From this expectation, we estimated the expected amount of BDM epistasis (equations (10) and (11)). These formulae assume that BDM loci interacting pairs are unlinked and segregate independently.

$$E(\bar{\omega}_{\mathrm{BDM_{HOME}}}) = \frac{\sum_{p1}^{p2} \sum_{i=1}^{n_{\mathrm{BDM\ pairs}}} (2 \times E(AABB_i)) + (2 \times E(AABb_i)) + (2 \times E(AaBb_i)) + (2 \times E(AaBb_i))}{2} \tag{10}$$

$$E(\bar{\omega}_{\mathrm{BDM_{AWAY}}}) = \sum_{i=1}^{n_{\mathrm{BDM\ pairs}}} (2 \times E(AABB_i)) + (2 \times E(AABb_i)) + (2 \times E(AaBB_i)) + (2 \times E(AaBb_i)) \tag{11}$$

After all the average fitness values were compiled, an estimated RI score was calculated using equation (12). This RI score represents the average fold higher fitness in the home population compared with the other (away) population. If there is no RI or populations are completely admixed, RI will equal 1, representing equal fitness in either environment.

$$\overline{\mathrm{RI}} = (1 - s_{\mathrm{RI}})^{(E(\bar{\omega}_{\mathrm{BDM_{AWAY}}}) + E(\bar{\omega}_{\mathrm{EX_{AWAY}}}))} / (1 - s_{\mathrm{RI}})^{(E(\bar{\omega}_{\mathrm{BDM_{HOME}}}) + E(\bar{\omega}_{\mathrm{EX_{HOME}}}))} \tag{12}$$

Selection coefficient visualization. To understand the scale of fitness effects in the simulation, we collected individual genotype values and sample fitness for each sample in each generation during the climate shift period (that is, generations 10,001 to 10,100). We then calculated s using equation (13). This equation compares the mean fitness for samples homozygous for the mutation with that of samples homozygous for the wild-type allele and is normalized by the mean fitness for wild-type samples. We required each group to have at least two individuals for s to be calculated.

$$s = (\bar{w}_{11} - \bar{w}_{00})/\bar{w}_{00} \tag{13}$$

In this case, s is the realized fitness effect, which includes the effect of linked loci. We plotted mutations with intermediate allele frequencies ($0.1 <$ frequency < 0.9) because at frequencies closer to 0 and 1, mutations are most often found in first-generation migrants and have more extreme variation in fitness (Fig. 1d).

Data availability
The authors declare that data supporting the findings of this study are available within the article, its supplementary information files and at https://github.com/owensgl/adaptive_introgression.

Code availability
All code for the underlying simulations is available at https://github.com/owensgl/adaptive_introgression.

References
25. Haller, B. C. & Messer, P. W. SLiM 3: forward genetic simulations beyond the Wright–Fisher model. *Mol. Biol. Evol.* **36**, 632–637 (2018).
26. Bateson, W. in *Darwin and Modern Science* (ed. Seward, A. C.) 85–101 (Cambridge Univ. Press, 1909).
27. Dobzhansky, T. H. Studies on hybrid sterility. II. Localization of sterility factors in *Drosophila pseudoobscura* hybrids. *Genetics* **21**, 113–115 (1936).
28. Muller, H. J. Isolating mechanisms, evolution, and temperature. *Biol. Symp.* **6**, 71–125 (1942).
29. Gingerich, P. D. Quantification and comparison of evolutionary rates. *Am. J. Sci.* **293**, 453–478 (1993).
30. R Core Team *R: A Language and Environment for Statistical Computing* (R Foundation for Statistical Computing, 2018); https://www.R-project.org/
31. Wickham, H. *ggplot2: Elegant Graphics for Data Analysis* (Springer, 2016)

Author contributions
G.O. and K.S. designed the study, created the model, analysed the results and wrote the paper.

Competing interests
The authors declare no competing interests.

Additional information
Supplementary information is available for this paper at https://doi.org/10.1038/s41558-019-0628-0.

Correspondence and requests for materials should be addressed to G.L.O.

Peer review information *Nature Climate Change* thanks Simon Martin, Joshua Miller and the other, anonymous, reviewer(s) for their contribution to the peer review of this work.

Reprints and permissions information is available at www.nature.com/reprints.